

Supplementary Information

Putting Together the Puzzle of Ion Transfer in Single-Digit Carbon Nanotubes: Ab Initio Meets Mean-Field

¹ Vadim Neklyudov[†] and Viatcheslav Freger^{*,†,‡,¶}

[†]*Wolfson Department of Chemical Engineering, Technion - IIT, Haifa 32000, Israel*

[‡]*Russel Berrie Nanotechnology Institute, Technion - IIT, Haifa 32000, Israel*

[¶]*Grand Technion Energy Program, Technion - IIT, Haifa 32000, Israel*

E-mail: vfreger@technion.ac.il

Phone: +972 (0) 4 829 2933

² Computation of hydration and transfer energies

³ The cycles for computing the thermodynamics quantities for hydration of water and ionic
⁴ species in water bulk, which is used for benchmarking the *ab initio* computations, and
⁵ transfer of ions and ion pairs from water to CNTs are schematically presented in Figure S1.
⁶ The excess quantities for hydration of a water molecule ($\Delta X_{aq}[\text{H}_2\text{O}]$) and ions ($\Delta X_{eq}[\text{Ion}]$)
⁷ in aqueous bulk relative to vacuum, where X is either E (electronic energy), H , G^{ex} , or S^{ex} ,
⁸ were calculated from computed X of corresponding single species in vacuum and in water
⁹ clusters as follows:

$$\Delta X_{aq}[\text{H}_2\text{O}] = 1/n \cdot X[(\text{H}_2\text{O})_n] \quad (1)$$

$$\Delta X_{aq}[\text{Ion}] = X[\text{Ion}(\text{H}_2\text{O})_n] - X[\text{Ion}] - n\Delta X_{aq}[\text{H}_2\text{O}]. \quad (2)$$

11 The equations for calculating the transfer energies of individual ions and ion pairs from water to CNTP are presented in the main text (see eqs. 9 and 10).

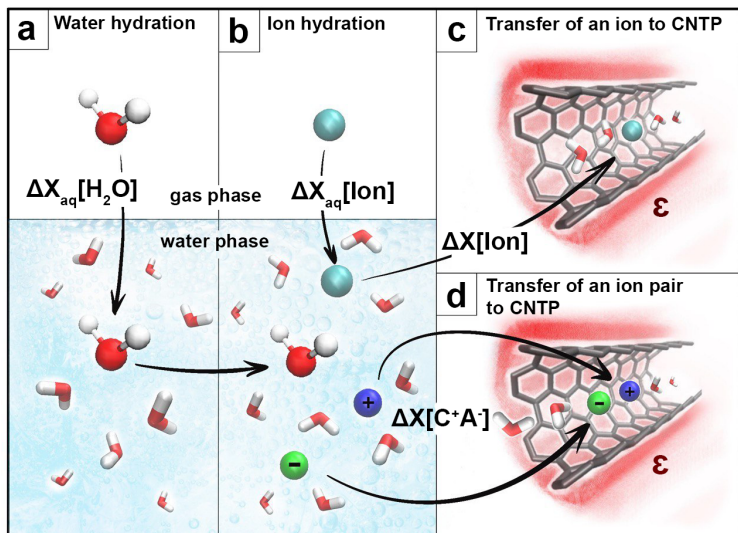


Figure S1: Thermodynamic cycles for computing energies of water hydration (a), ion hydration (b) and transfer of an ion (c) or an ion pair (d) to CNTP. An ion and carbon, oxygen, and hydrogen atoms are cyan, grey, red, and white, respectively; positive and negative ions are presented as blue and green. Water clusters with and without an ion are embedded in a polarizable continuum with dielectric constant 78.36 representing bulk water. The CNTPs are surrounded by a continuum of dielectric constant ϵ .

13 **Benchmarking of hydration energies and interaction with benzene**

14 Figure S2a compares the computed thermodynamic quantities for hydration of water and
 15 ions with experimental values. It demonstrates that the selected level of theory (wB97XD/6-
 16 31G(d,p)) adequately reproduces the hydration thermodynamics. Figure S2b demonstrates
 17 a comparison of the experimental and calculated values of the enthalpies of interaction of
 18 water and potassium ion with benzene, as a surrogate model of the nanotube wall, showing
 19 a reasonable agreement a well.

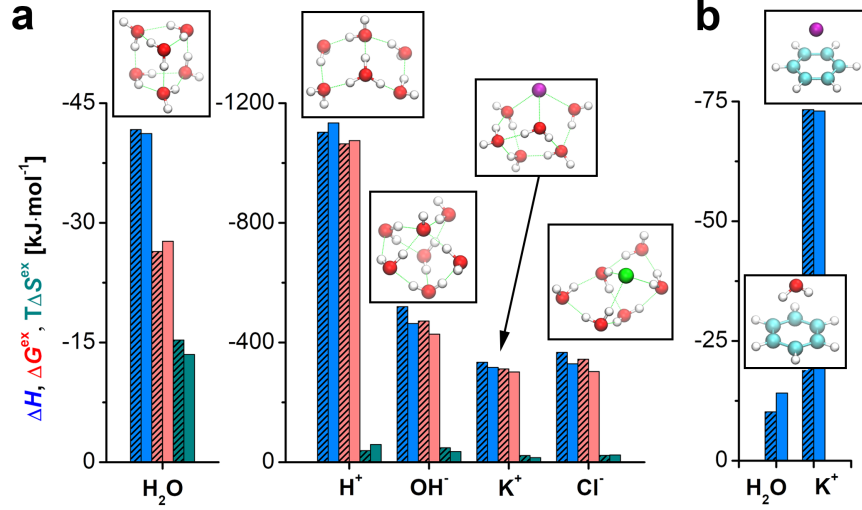


Figure S2: (A) The benchmarking of calculated hydration energies (non-shaded bars) of H_2O , H^+ , OH^- , K^+ and Cl^- with their experimental values (shaded bars). Blue, red and dark green bars are enthalpies, excess Gibbs energies and entropies, respectively. The optimized clusters embedded into IEFPCM model are also presented. (B) Experimental and calculated enthalpies of benzene complex with H_2O and K^+ . All energies are obtained under standard conditions (298.15 K, 1 bar). The experimental values are from *Y. Marcus John Wiley & Sons, 2015*¹

20 Derivation of the relation for CNTP conductance

21 The derivation is for the case when both ion uptake and conductance are controlled by free
 22 potassium and hydroxide ions, eq. 4 in the main text. Further, the assumption of a local
 23 mean-field electric potential is used, while this potential may vary along CNTP. The total
 24 steady-state current I flowing through the CNTP sums up the currents carried by each ion,
 25 which can be related to the gradients of the electric potential and ion concentrations using
 26 the following Nernst-Planck equation

$$\frac{I}{F} = \frac{I_K + I_{OH}}{F} = -\bar{D}_K \bar{C}_K (\nabla \ln C_K + \nabla \phi) + \bar{D}_{OH} \bar{C}_{OH} (\nabla \ln C_{OH} - \nabla \phi), \quad (3)$$

27 where I_i , \bar{D}_i and \bar{C}_i are, respectively, the current, diffusion (mobility) coefficient, and local
 28 concentration of species i within CNTP and the signs before different terms account for
 29 ion charges. The expressions in brackets are driving forces made up of chemical and elec-
 30 tric potential gradients, where C_i (no bar) should be understood as respective equilibrium

31 concentrations in solution. To make the notation compact, here \bar{C}_i are taken as linear con-
 32 centrations obtained by multiplying volume concentrations in the channel by the channel
 33 cross-section area πr_c^2 , where r_c is the channel radius, and potential ϕ is dimensionless, in
 34 units of thermal potential RT/F .

35 Local electroneutrality within CNTP implies $\bar{C}_{OH} = \bar{C}_K = \alpha(C_K C_{OH})^{1/2}$, where $\alpha =$
 36 $\pi r_c^2 \exp\left(-\frac{\Delta G_K^{ex} + \Delta G_{OH}^{ex}}{2RT}\right)$ plays the role of the partitioning coefficient (cf. eq. 3 in the paper).
 37 The expressions for currents of individual ions I_K and I_{OH} may then be recast as follows

$$\frac{I_K}{\alpha F \bar{D}_K} (C_K C_{OH})^{-1/2} = -\nabla \ln C_K - \nabla \phi, \quad (4)$$

38

$$\frac{I_{OH}}{\alpha F \bar{D}_{OH}} (C_K C_{OH})^{-1/2} = +\nabla \ln C_{OH} - \nabla \phi. \quad (5)$$

39 After subtracting eq. 5 from eq. 4 and multiplying by $(C_K C_{OH})^{1/2}$, we obtain

$$\frac{1}{\alpha F} \left(\frac{I_K}{D_K} - \frac{I_{OH}}{D_{OH}} \right) = -(C_K C_{OH})^{1/2} \nabla \ln (C_K C_{OH}) = -2 \nabla (C_K C_{OH})^{1/2} \quad (6)$$

40 Since all terms at the l.h.s. of eq. 6 are constant, it may be integrated to derive the linear
 41 variation of $(C_K C_{OH})^{1/2}$ along the CNTP (coordinate $0 \leq x \leq L$)

$$(C_K C_{OH})^{1/2} = (C_K C_{OH})_{x=0}^{1/2} - \frac{1}{2\alpha F} \left(\frac{I_K}{D_K} - \frac{I_{OH}}{D_{OH}} \right) x = (C_K C_{OH})_{x=0}^{1/2} + \frac{x}{L} \Delta (C_K C_{OH})^{1/2}, \quad (7)$$

42 which also indicates that the r.h.s. of eq. 6 is simply $-2\Delta(C_K C_{OH})^{1/2}/L$. (Here and below
 43 Δ designates the difference between the two solutions connected with CNTP.)

44 Conversely, after adding up eqs. 4 and 5 and integrating over the entire CNTP length,
 45 we obtain

$$\frac{1}{\alpha F} \left(\frac{I_K}{\bar{D}_K} + \frac{I_{OH}}{\bar{D}_{OH}} \right) = \frac{1}{\beta} [-2\Delta\phi - \Delta \ln C_K + \Delta \ln C_{OH}], \quad (8)$$

46 where $\beta = \int_0^L (C_{OH}C_K)^{-1/2} dx$. Equation 7 can be used to obtain β

$$\beta = \frac{L}{\Delta(C_{OH}C_K)^{1/2}} \int_0^L d \ln(C_{OH}C_K)^{1/2} = L \frac{\Delta \ln(C_{OH}C_K)^{1/2}}{\Delta(C_{OH}C_K)^{1/2}} = \frac{L}{\langle (C_{OH}C_K)^{1/2} \rangle_{l.m.}}. \quad (9)$$

47 Finally, we define ion transport numbers $t_K = \frac{\bar{D}_K}{\bar{D}_K + \bar{D}_{OH}}$ and $t_{OH} = \frac{\bar{D}_{OH}}{\bar{D}_K + \bar{D}_{OH}} = 1 - t_K$ and
 48 use the relation $I_{OH} = I - I_K$ to combine eqs 6, 8, and 9, find I_K and I_{OH} and obtain eq. 10

$$I = I_K + I_{OH} = G [-\Delta\phi - t_K \Delta \ln C_K + t_{OH} \Delta \ln C_{OH}], \quad (10)$$

49 where the expression in square brackets defines the total potential difference driving the
 50 current and the effective CNTP conductance is given by

$$G = \frac{\alpha F (\bar{D}_K + \bar{D}_{OH})}{\beta} = \frac{\alpha F (\bar{D}_K + \bar{D}_{OH})}{L} \langle (C_{OH}C_K)^{1/2} \rangle_{l.m.} \quad (11)$$

51 When the potential is expressed in Volts, eq. 11 should be multiplied by F/RT to obtain
 52 conductance in Siemens. It is easy to see that, when the product $C_{OH}C_K$ largely differs
 53 for the two solutions, the conductance is mainly controlled by the solution with the larger
 54 $C_{OH}C_K$.

55 **Thermodynamics parameters for ions and ion pairs obtained from** 56 ***ab initio* calculations**

57 Table S1 presents thermodynamics data for the transfer of single ionic species within CNT(6,6)
 58 and CNT(5,5). The results for CNT(6,6) include results the zigzag and triple-bonded (3-
 59 bonded) arrangement of water. Fig. S3 presents the same data as bar diagrams to facilitate
 60 comparison with Fig. 1f in the main text.

Table S2: The transfer energies (ΔG^{ex} , ΔH , $-T\Delta S^{ex}$) of species under consideration at different dielectric constants outside CNT(6,6) and (5,5) (in parenthesis) calculated at wB97X-D/6-31G(d,p). From left to right: CNT(6,6) 3-bonded / CNT(6,6) zigzag / CNT(5,5)

Species	$\epsilon = 1$	$\epsilon = 2$	$\epsilon = 100$
Excess Gibbs transfer energies (ΔG^{ex})			
H ₂ O	20.5/-15.8/-8.8	19.7/-17.3/-10.4	21.4/-18.2/-10.5
H ⁺	40.0/29.9/93.5	7.4/-3.8/50.8	-33.7/-71.3/16.8
OH ⁻	177.7/167.6/202.4	130.3/119.0/151.6	60.7/23.1/93.0
K ⁺	49.6/39.5/53.2	6.1/-5.1/9.9	-52.0/-89.6/-22.8
Cl ⁻	189.5/179.4/190.1	133.1/121.8/128.7	62.7/25.1/62.6
Enthalpy of transfer (ΔH)			
H ₂ O	14.4/-17.9/5.4	16.0/-16.5/6.2	20.1/-14.1/8.4
H ⁺	32.3/3.8/93.1	-0.3/-38.1/50.0	-41.2/-130.7/16.5
OH ⁻	169.4/140.8/208.8	122.4/84.6/58.7	52.7/-36.8/99.9
K ⁺	43.5/15.0/41.4	0.7/-37.1/-1.2	-56.6/-146.2/-33.2
Cl ⁻	166.3/137.8/186.8	121.7/83.8/137.3	57.7/-31.9/77.5
Excess entropy of transfer ($-T\Delta S^{ex}$)			
H ₂ O	6.1/2.1/-14.2	3.6/-0.8/-16.6	1.3/-4.1/-18.9
H ⁺	7.7/26.1/0.5	7.7/34.3/0.8	7.4/59.4/0.3
OH ⁻	8.4/26.8/-6.4	7.8/34.4/-7.1	7.9/59.8/-6.9
K ⁺	6.1/24.5/11.8	5.4/32.0/11.1	4.6/56.5/10.4
Cl ⁻	23.2/41.5/3.3	11.4/38.0/-8.5	5.0/56.9/-14.9

61 **Fitting of transfer excess Gibbs energies to experimental data on**
62 **conductivity and anion permeation in vesicles**

63 The data presented in Figure 2a were fitted to the above equation for conductivity for pH
64 7.5, eq. 11, which was recast in the following form

$$G(\text{pH } 7.5) = \frac{F^2}{RT} \frac{\pi r_c^2}{L} (\bar{D}_K + \bar{D}_{OH})(C_{OH}C_K)^{1/2} \exp\left(-\frac{\Delta G_h^{ex}}{RT}\right) \quad (12)$$

65 Dellago et al.² computed the values of diffusivity in CNTP for water (as water defects in
66 single file) and proton (by Grotthuss mechanism) 40 and 170×10^{-8} m²/s, respectively. We
67 use the former as an estimate of \bar{D}_K and correct the latter by the ratio of bulk diffusivities
68 of hydroxide and proton in water $D_{OH}/D_H = 0.5$ to estimate $\bar{D}_{OH} = 85 \times 10^{-8}$. For pH

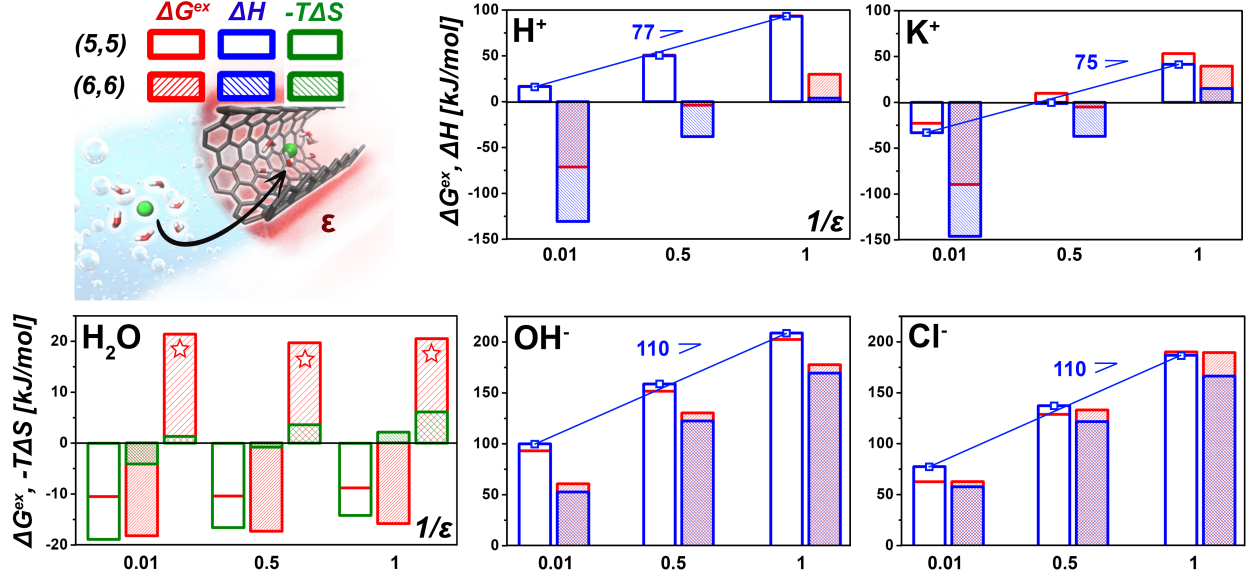


Figure S3: The transfer quantities for water and ions in (5,5) CNTP. For water transfer, the stars indicate triple-bonded water arrangement inside (6,6) CNTP. The slopes represent the dielectric energy.

69 7.5, i.e., $C_{OH} = 10^{-6.5}$ M, the conductivity shows a linear dependence on $(C_s C_{OH})^{1/2}$. Using
70 $L = 10.6$ nm and van der Waals radius of CNTP(6,6) $r_c = 0.68$ nm, G_h^{ex} is viewed as the
71 only adjustable parameter, computed from the slope of the fitted linear dependence passing
72 through the origin (zero intercept) to obtain $G_h^{ex} = -6$ kJ/mol.

73 The analogous relation for pH 3 is

$$G(\text{pH } 3) = \frac{F^2}{RT} \frac{\pi r_c^2}{L} (\bar{D}_K + \bar{D}_{Cl}) C_s \exp\left(-\frac{\Delta G_s^{ex}}{RT}\right) \quad (13)$$

74 Using estimates $\bar{D}_K = \bar{D}_{Cl} = 4 \times 10^{-8}$ m²/s, the slope fitted to linear dependence of G on
75 C_s yield $G_s^{ex} = 14$ kJ/mol.

76 In a similar manner, we fitted to the experimental chloride permeation rate Q_{Cl} at pH 7
77 in Fig. 2b to the relation

$$Q_{Cl}(\text{pH } 7.5) = \frac{\pi r_c^2}{L} \bar{D}_{Cl} C_s^{3/2} C_{OH}^{-1/2} \exp\left(-\frac{\Delta \tilde{G}_s^{ex}}{RT}\right), \quad (14)$$

78 The chloride transfer rate per CNTP in Fig. 2b was computed from the digitised row data

79 for chloride flux in vesicles reported by Li et al.³ and rescaled using the factor based on
 80 the chloride permeability reported in this paper. The the best fit to eq. 14 yielded the
 81 value $\Delta\tilde{G}_s^{ex} = 50$ kJ/mol presented in Fig. 2b. Figure S4 presents row data from Li et al.
 82 scaled in 3 different ways. This demonstrates that, while the plot of chloride flux versus $C_s^{3/2}$
 83 shows a good linear relation with zero intercept (panel b), the plots versus C_s and C_s^2 show
 84 a non-linear dependence, with a non-zero-intercept for linear fits.

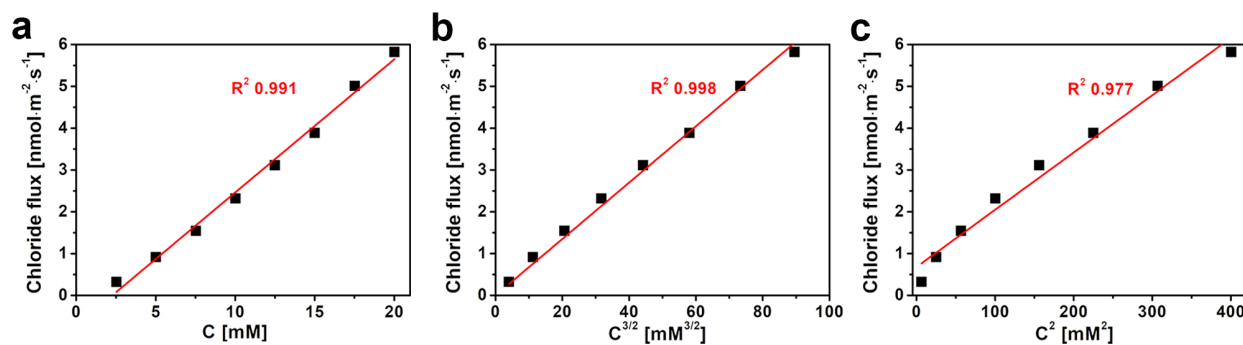


Figure S4: Chloride flux as a function of salt concentration. The data points were digitized from Li et al.³

85 References

- 86 (1) Marcus, Y. *Ions in Solution and their Solvation*; John Wiley & Sons, 2015.
- 87 (2) Dellago, C.; Naor, M. M.; Hummer, G. Proton transport through water-filled carbon
 88 nanotubes. *Phys. Rev. Lett.* **2003**, *90*, 105902.
- 89 (3) Li, Y.; Li, Z.; Aydin, F.; Quan, J.; Chen, X.; Yao, Y.-C.; Zhan, C.; Chen, Y.;
 90 Pham, T. A.; Noy, A. Water-ion permselectivity of narrow-diameter carbon nanotubes.
 91 *Sci. Adv.* **2020**, *6*, eaba9966.